

## The antithrombotic potential of selective blockade of talin-dependent integrin $\alpha_{IIb}\beta_3$ (platelet GPIIb–IIIa) activation

Brian G. Petrich, ... , Sanford J. Shattil, Mark H. Ginsberg

*J Clin Invest.* 2007;117(8):2250–2259. <https://doi.org/10.1172/JCI31024>.

Research Article

Hematology

In vitro studies indicate that binding of talin to the  $\beta_3$  integrin cytoplasmic domain (tail) results in integrin  $\alpha_{IIb}\beta_3$  (GPIIb–IIIa) activation. Here we tested the importance of talin binding for integrin activation in vivo and its biological significance by generating mice harboring point mutations in the  $\beta_3$  tail. We introduced a  $\beta_3$ (Y747A) substitution that disrupts the binding of talin, filamin, and other cytoplasmic proteins and a  $\beta_3$ (L746A) substitution that selectively disrupts interactions only with talin. Platelets from animals homozygous for each mutation showed impaired agonist-induced fibrinogen binding and platelet aggregation, providing proof that inside-out signals that activate  $\alpha_{IIb}\beta_3$  require binding of talin to the  $\beta_3$  tail.  $\beta_3$ (L746A) mice were resistant to both pulmonary thromboembolism and to ferric chloride–induced thrombosis of the carotid artery. Pathological bleeding, measured by the presence of fecal blood and development of anemia, occurred in 53% of  $\beta_3$ (Y747A) and virtually all  $\beta_3$ -null animals examined. Remarkably, less than 5% of  $\beta_3$ (L746A) animals exhibited this form of bleeding. These results establish that  $\alpha_{IIb}\beta_3$  activation in vivo is dependent on the interaction of talin with the  $\beta_3$  integrin cytoplasmic domain. Furthermore, they suggest that modulation of  $\beta_3$  integrin–talin interactions may provide an attractive target for antithrombotics and result in a reduced risk of pathological bleeding.

Find the latest version:

<https://jci.me/31024/pdf>





# The antithrombotic potential of selective blockade of talin-dependent integrin $\alpha_{IIb}\beta_3$ (platelet GPIIb–IIIa) activation

Brian G. Petrich, Per Fogelstrand, Anthony W. Partridge, Nima Yousefi, Ararat J. Ablooglu, Sanford J. Shattil, and Mark H. Ginsberg

Department of Medicine, UCSD School of Medicine, La Jolla, California, USA.

**In vitro studies indicate that binding of talin to the  $\beta_3$  integrin cytoplasmic domain (tail) results in integrin  $\alpha_{IIb}\beta_3$  (GPIIb–IIIa) activation. Here we tested the importance of talin binding for integrin activation in vivo and its biological significance by generating mice harboring point mutations in the  $\beta_3$  tail. We introduced a  $\beta_3$ (Y747A) substitution that disrupts the binding of talin, filamin, and other cytoplasmic proteins and a  $\beta_3$ (L746A) substitution that selectively disrupts interactions only with talin. Platelets from animals homozygous for each mutation showed impaired agonist-induced fibrinogen binding and platelet aggregation, providing proof that inside-out signals that activate  $\alpha_{IIb}\beta_3$  require binding of talin to the  $\beta_3$  tail.  $\beta_3$ (L746A) mice were resistant to both pulmonary thromboembolism and to ferric chloride-induced thrombosis of the carotid artery. Pathological bleeding, measured by the presence of fecal blood and development of anemia, occurred in 53% of  $\beta_3$ (Y747A) and virtually all  $\beta_3$ -null animals examined. Remarkably, less than 5% of  $\beta_3$ (L746A) animals exhibited this form of bleeding. These results establish that  $\alpha_{IIb}\beta_3$  activation in vivo is dependent on the interaction of talin with the  $\beta_3$  integrin cytoplasmic domain. Furthermore, they suggest that modulation of  $\beta_3$  integrin–talin interactions may provide an attractive target for antithrombotics and result in a reduced risk of pathological bleeding.**

## Introduction

Primary hemostasis following vascular injury is dependent on the aggregation of platelets and the formation of a platelet plug. In arterial disease, however, platelet aggregation can lead to an occlusive platelet thrombus, resulting in myocardial infarction or stroke. Platelet aggregation requires the binding of soluble multivalent adhesive ligands, such as fibrinogen, fibronectin, or von Willebrand factor to platelet GPIIb–IIIa (integrin  $\alpha_{IIb}\beta_3$ ). Indeed, blockade of ligand binding to  $\alpha_{IIb}\beta_3$  by agents such as abciximab, eptifibatid, or tirofiban can completely inhibit platelet aggregation. Thus, these agents are effective in the prevention and treatment of arterial thrombosis in the acute settings of percutaneous coronary intervention (1). In spite of the compelling mechanistic rationale for such pharmacological blockade of  $\alpha_{IIb}\beta_3$ , the chronic administration of oral  $\alpha_{IIb}\beta_3$  antagonists has not proved beneficial in preventing recurrent thrombotic events (2). One plausible explanation for this failure is the relatively narrow therapeutic window for these agents because pathological bleeding associated with complete loss of  $\alpha_{IIb}\beta_3$  function necessitates maintenance of less than maximal blockade of the integrin (1). Thus, the role of  $\alpha_{IIb}\beta_3$  in arterial thrombosis and the clinical success of acute blockade of this integrin indicate that it is a useful therapeutic target; however, the failure of oral  $\alpha_{IIb}\beta_3$  antagonists suggests that a better understanding of how this receptor functions in thrombosis and in prevention of pathological bleeding in vivo could lead to advantageous new approaches to therapeutic platelet inhibition.

Regulation of the affinity of  $\alpha_{IIb}\beta_3$  for adhesive ligands is central to the control of platelet aggregation (3).  $\alpha_{IIb}\beta_3$  is expressed in a low-

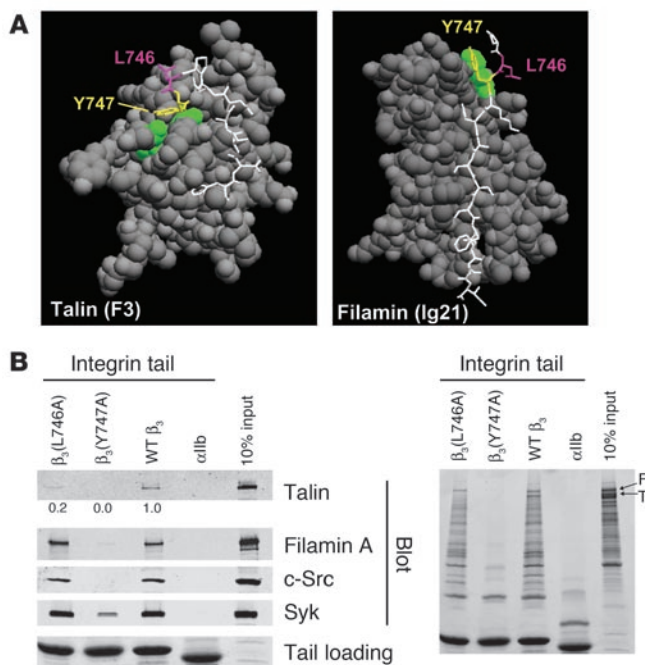
affinity form in resting platelets, and intracellular signals initiated by agonists, such as ADP or thromboxane  $A_2$ , acting via distinct receptors, result in increased affinity of  $\alpha_{IIb}\beta_3$ , often referred to as “activation” (4). Agents that block signaling through ADP receptors (e.g., clopidogrel) or through the generation of thromboxane  $A_2$  (e.g., aspirin) are moderately beneficial in the chronic prevention of arterial thrombosis (5), suggesting that more effective blockade of the activation of  $\alpha_{IIb}\beta_3$  might be a useful antithrombotic strategy.

Activation is an intrinsic property of the integrin  $\alpha_{IIb}\beta_3$  and can be due to changes in the conformation of the extracellular domain and/or to cooperative binding to multivalent ligands resulting from integrin clustering (6). Electron microscopic and immunochemical analyses suggest that long-range changes in the tertiary and quaternary structures of integrins also contribute to affinity regulation; however, the full range of these conformational changes remains to be determined (7–9). Recent in vitro analyses, using model systems, indicate that the binding of talin to the cytoplasmic domain of  $\beta_3$  integrin and other integrin cytoplasmic domains is a final common step in integrin activation (10–12), and they have defined critical structural features of the interaction (13). Taking into consideration insights from these structural studies, we have generated mice with mutations in the mouse  $\beta_3$  integrin tail that selectively disrupt the binding of talin alone or the binding of talin and several other cytoplasmic proteins to  $\beta_3$  in platelets. We find that binding of talin to the  $\beta_3$  integrin tail is critical for agonist-induced  $\alpha_{IIb}\beta_3$  activation in vivo. More importantly, we demonstrate that selective disruption of the  $\beta_3$  integrin–talin interaction protects mice from thrombosis without causing the anemia and gastrointestinal (GI) bleeding associated with the complete loss of  $\beta_3$  integrin function in  $\beta_3$ -null mice. These data suggest that disrupting the  $\beta_3$ -talin interaction may offer antithrombotic benefit by widening the therapeutic window of  $\alpha_{IIb}\beta_3$  antagonism.

**Nonstandard abbreviations used:** GI, gastrointestinal.

**Conflict of interest:** The authors have declared that no conflict of interest exists.

**Citation for this article:** *J. Clin. Invest.* 117:2250–2259 (2007). doi:10.1172/JCI31024.

**Figure 1**

Structure-based mutagenesis of the  $\beta_3$  integrin cytoplasmic domain. **(A)** Space-filled models of talin F3 domain (left) or filamin A immunoglobulin-like domain 21 in complex with short internal fragments of the  $\beta_3$  integrin cytoplasmic domain (shown as sticks, with Tyr747 and Leu746 in yellow and purple, respectively). **(B)** Affinity chromatography using recombinant WT and mutant  $\beta_3$  cytoplasmic domain proteins and mouse platelet lysates as described in Methods. Bound platelet proteins were analyzed by Western blotting with the indicated antibodies (left panel) and by Coomassie blue staining (right panel). Quantitation of the amount of talin bound in mutant relative to WT platelets is shown. Similar results were obtained from 2 independent experiments. F, filamin; T, talin.

## Results

**Integrin  $\beta_3$  cytoplasmic domain mutants that disrupt interactions with platelet intracellular proteins.** Previous *in vitro* studies with human proteins pointed to  $\beta_3$ (Tyr747) and  $\beta_3$ (Leu746) as potential targets for disrupting the intracellular interactions of the  $\beta_3$  cytoplasmic domain with talin (13, 14). The crystal structure of  $\beta_3$  residues Trp739 to Tyr747 in complex with talin F3 shows that both  $\beta_3$ (Tyr747) and  $\beta_3$ (Leu746) make extensive contacts with talin. In contrast, a homology model of  $\beta_3$  (Pro745 to Ile757) docked into the structure of filamin A immunoglobulin-like domain 21 predicted hydrophobic contacts between  $\beta_3$ (Tyr747) and a loop between 2  $\beta$  strands in filamin A. However, in contrast to what occurs in the integrin-talin interaction,  $\beta_3$ (Leu746) makes no contacts with filamin A (Figure 1A). These structures explain why  $\beta_3$ (Y747A) blocks the binding of both human talin and filamin, whereas  $\beta_3$ (L746A) blocks only talin binding (12). To test the role of  $\beta_3$ (Tyr747) and  $\beta_3$ (Leu746) on the binding of proteins from murine platelet lysates, we used recombinant WT and mutant  $\beta_3$  integrin cytoplasmic domain proteins in affinity chromatography experiments. WT  $\beta_3$  bound mouse talin and filamin. In addition, the  $\beta_3$  cytoplasmic domain bound the tyrosine kinases Syk and c-Src (Figure 1B, left panel).  $\beta_3$ (Y747A) disrupted interactions with each of these mouse proteins. In sharp contrast, although  $\beta_3$ (L746A) bound much less talin than WT  $\beta_3$ , it bound other proteins to the same extent as WT  $\beta_3$ . Inspection of protein-stained gels underscored the specificity of the effect of the  $\beta_3$ (L746A) mutation on protein binding; there was no substantial reduction in any of the  $\beta_3$ -binding proteins other than talin (Figure 1B, right panel). These results indicate that both  $\beta_3$ (Y747A) and  $\beta_3$ (L746A) mutations disrupt  $\beta_3$ -talin interactions in mouse platelets. However,  $\beta_3$ (Y747A) blocks binding of many other proteins, probably because it disrupts the  $\beta$  turn formed by N<sup>744</sup>PLY (15) in addition to disrupting direct contacts with the protein ligands. Thus, the effects of these point mutations on the binding of murine proteins to the  $\beta_3$  cytoplasmic domain enable us to evaluate the effects on

murine platelet function of selective blockade of talin binding versus a more general blockade of protein interactions.

**Generation of mice bearing  $\beta_3$ (Y747A) and  $\beta_3$ (L746A) mutations.** To test the effects of  $\beta_3$ (Y747A) and  $\beta_3$ (L746A) mutations on platelet function, we generated mice harboring either of these mutations using a gene-targeting approach similar to that previously described for the construction of the  $\beta_3$ (Y747,759F) integrin subunit (16). Mouse 129/SvJ ES cells were electroporated with a targeting vector containing 6 kb of  $\beta_3$  genomic sequence, a *loxP*-flanked neomycin (Neo) cassette inserted between exons 14 and 15, and either Y747A or L746A mutation in exon 15 (Figure 2A). ES clones were screened by PCR and confirmed by Southern blotting using cDNA probes 5' and 3' to the targeted sequence (Figure 2B) and with a Neo probe to confirm a single integration site of the targeting vector (data not shown). For each mutation, 2 independently derived clones of ES cells were injected into C57BL/6 blastocysts. Each ES cell clone generated chimeric mice that exhibited germline transmission of the mutation as determined by PCR (data not shown). Heterozygous animals were crossed with EIIIa-Cre mice to obtain offspring in which the Neo cassette was excised. Heterozygous animals were crossed to obtain animals homozygous for the mutations or WT littermates as determined by PCR on genomic DNA isolated from ear biopsy samples (Figure 2C). The presence of the mutation in  $\beta_3$  integrin mRNA was confirmed by sequencing reverse transcription-polymerase chain reaction products generated using RNA isolated from spleens of homozygous mutant animals. Mice were backcrossed to a C57BL/6 strain for at least 3 generations, and WT sex-matched littermates were used as controls for homozygous mutant animals in all experiments. Similar to  $\beta_3$ -null animals (17), these mutant mice exhibited no gross developmental abnormalities and had normal platelet and white blood cell counts (Table 1). Thus, the mice are suitable for examination of blocking interactions of the  $\beta_3$  cytoplasmic domain on platelet function *in vivo* and *in vitro*.

**Protection from thrombosis in  $\beta_3$ (Y747A) and  $\beta_3$ (L746A) mice.** Since  $\alpha_{IIb}\beta_3$  is required for platelet aggregation, we examined the effect of the  $\beta_3$ (Y747A) and  $\beta_3$ (L746A) mutations on the formation of occlusive platelet thrombi in a pulmonary thromboembolism model in which platelet activation was induced by tail vein infusion of collagen and epinephrine. Upon intravenous injection of a mixture of these platelet agonists, 64% of WT littermates (20 of 31 mice) died within 5 minutes (Figure 3A). Histological examination of lung tissue from these animals revealed platelet thrombi throughout the pulmonary vasculature (Figure 3B). In sharp contrast, 100% of  $\beta_3$ (Y747A) (12 of 12 mice) and 95% of  $\beta_3$ (L746A) (15 of 16 mice) animals survived the infusion of collagen and epinephrine ( $P < 0.005$ ,

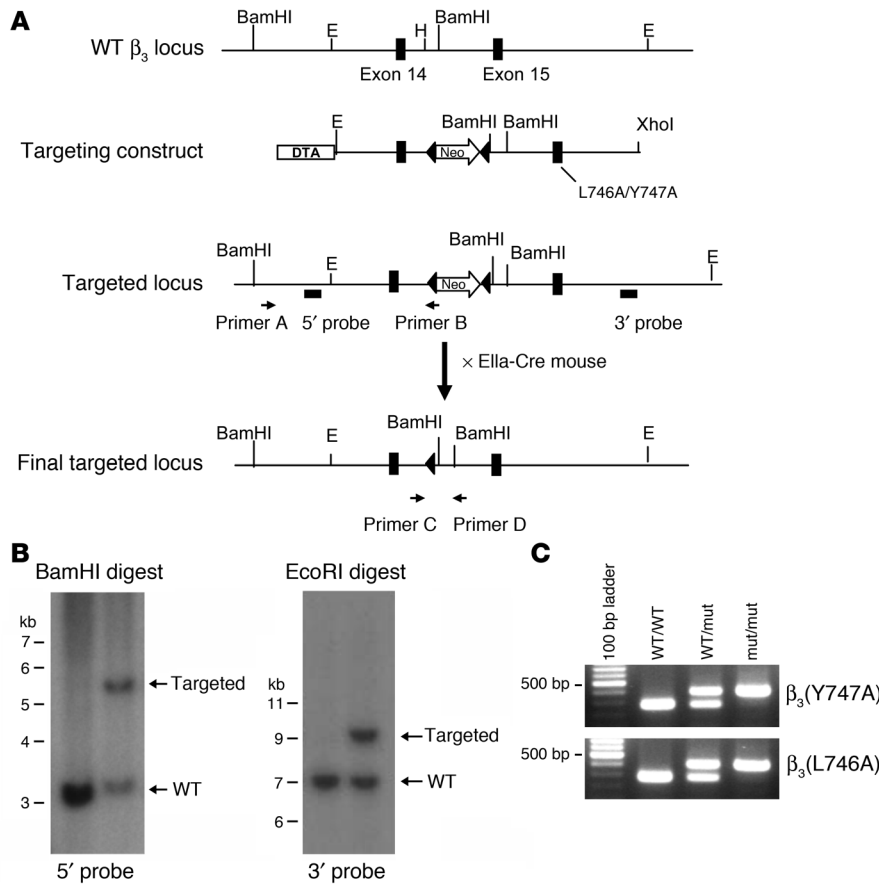


**Figure 2**

Generation of  $\beta_3$ (Y747A) and  $\beta_3$ (L746A) mutant mice. **(A)** Targeting vector containing 6 kb of the 3' end of the mouse  $\beta_3$  integrin gene (exons 14 and 15). Tyr747- and Leu746-to-alanine mutations were inserted into exon 15. DTA, diphtheria toxin A. **(B)** Southern blot analysis of R1 ES cell genomic DNA transfected with the  $\beta_3$ (Y747A) targeting vector with BamHI (left) or EcoRI (right) using a 5' probe or 3' probe, respectively. **(C)** PCR genotyping of genomic DNA isolated from  $\beta_3$ (Y747A) and  $\beta_3$ (L746A) mouse ear biopsy samples using primers C and D shown in **A**. H, HindIII; E, EcoRI.

able blood in their stool (Figure 5A). In contrast, fewer  $\beta_3$ (Y747A) animals (19 of 36) were positive for fecal blood, indicating that  $\beta_3$ (Y747A) impairs vascular integrity to a lesser extent than complete lack of  $\beta_3$ . In sharp contrast to the results in null and  $\beta_3$ (Y747A) mice, less than 5% of  $\beta_3$ (L746A) animals (1 of 23) exhibited fecal blood. The protection from GI bleeding in the  $\beta_3$ (L746A) mice was confirmed by their lack of anemia relative to the  $\beta_3$ (Y747A) animals (Figure 5B and Table 1). Indeed,  $\beta_3$ (L746A) mice showed hematocrits and hemoglobin levels similar to those of WT animals. The pathological bleeding observed in  $\beta_3$ (Y747A) mice was associated with reduced prenatal

and perinatal survival. Significantly fewer homozygous  $\beta_3$ (Y747A) mutant animals obtained from heterozygote by heterozygote breedings survived to weaning age (144 homozygotes versus 192 WT;  $P < 0.00001$ ).  $\beta_3$ (L746A) animals, however, were observed at expected Mendelian ratios (106 homozygotes versus 108 WT;  $P = 0.97$ ). Together, these results indicate that  $\beta_3$ (Y747A) animals display a

WT versus either mutant; Figure 3A). The lungs of these mutant mice were largely devoid of platelet thrombi (Figure 3B). To examine the effects of the  $\beta_3$ (L746A) mutations in a model of arterial thrombosis initiated by vascular injury, we measured the time course of thrombus formation in response to ferric chloride-induced injury of the common carotid artery. In this model, the carotid arteries of 6 of 6 WT mice completely occluded in an average of  $6.4 \pm 1.9$  minutes following injury (Figure 4A). In contrast, arteries of 0 of 5  $\beta_3$ (L746A) mice occluded during the 30 minutes following injury despite similar levels of ferric chloride-induced endothelial damage (Figure 4, A and B). Thus,  $\beta_3$ (L746A) mice are protected from thrombosis in models involving impact to large arteries or the microcirculation.

*Reduced GI bleeding in  $\beta_3$ (L746A) mice.* Mice entirely lacking integrin  $\beta_3$  exhibit GI bleeding associated with reduced survival (17). Indeed, in our hands 100% (11 of 11) of  $\beta_3$ -null animals had detect-

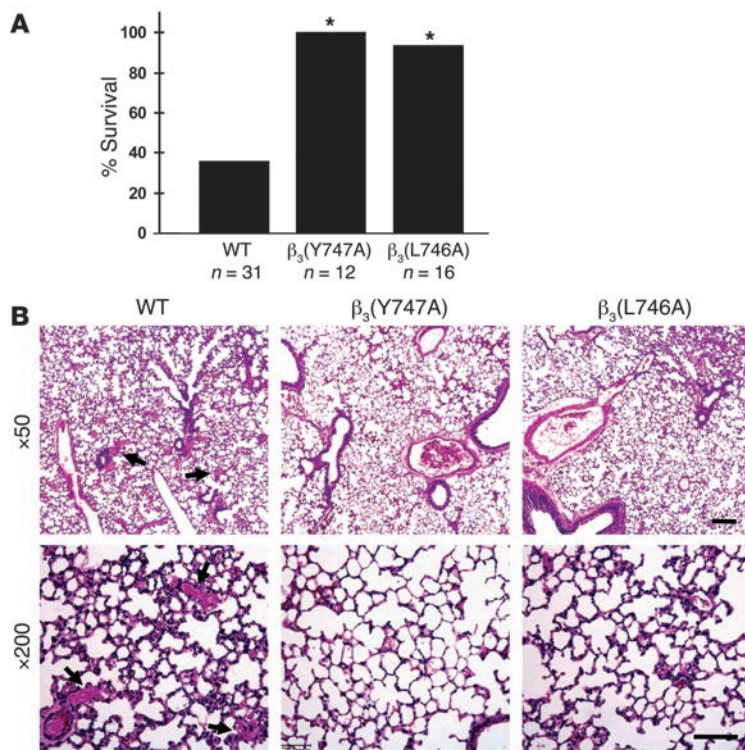
able blood in their stool (Figure 5A). In contrast, fewer  $\beta_3$ (Y747A) animals (19 of 36) were positive for fecal blood, indicating that  $\beta_3$ (Y747A) impairs vascular integrity to a lesser extent than complete lack of  $\beta_3$ . In sharp contrast to the results in null and  $\beta_3$ (Y747A) mice, less than 5% of  $\beta_3$ (L746A) animals (1 of 23) exhibited fecal blood. The protection from GI bleeding in the  $\beta_3$ (L746A) mice was confirmed by their lack of anemia relative to the  $\beta_3$ (Y747A) animals (Figure 5B and Table 1). Indeed,  $\beta_3$ (L746A) mice showed hematocrits and hemoglobin levels similar to those of WT animals. The pathological bleeding observed in  $\beta_3$ (Y747A) mice was associated with reduced prenatal

**Table 1**  
Hemograms for WT and  $\beta_3$  mutant mice

	$\beta_3$ (L746A)				$\beta_3$ (Y747A)			
	WT		Homozygous		WT		Homozygous	
	Mean	SEM	Mean	SEM	Mean	SEM	Mean	SEM
wbc ( $\times 10^9/l$ )	4.2	0.4	3.2	0.3	4.2	0.9	2.6	0.3
rbc ( $\times 10^9/l$ )	9.0	0.1	8.2 <sup>A</sup>	0.2	9.1	0.2	6.8 <sup>A</sup>	0.4
Hemoglobin (g/l)	13.9	0.1	13.3	0.3	13.8	0.3	10.8 <sup>A</sup>	0.6
Hematocrit (%)	49.1	0.7	46.7	1.1	48.4	0.6	39.8 <sup>A</sup>	2.2
MCV (fl)	54.4	0.6	56.8	1.3	53.5	0.8	58.5 <sup>A</sup>	0.9
MCH (pg)	15.4	0.1	16.2 <sup>A</sup>	0.2	15.2	0.1	16.0 <sup>A</sup>	0.3
MCHC (g/dl)	28.4	0.3	28.6	0.5	28.5	0.5	27.4	0.5
Platelets ( $\times 10^9/l$ )	618	57	616	57	633	69	689	51
Neutrophils (%)	41.5	3.8	39.8	5.7	32.5	4.0	36.7	5.0
Lymphocytes (%)	47.9	4.4	50.5	6.4	53.1	4.5	53.4	5.4
Monocytes (%)	6.8	1.1	6.5	1.0	9.5	1.0	7.2	0.9
Eosinophils (%)	3.4	0.7	3.3	0.8	5.1	1.1	2.8	0.9

<sup>A</sup> $P < 0.05$  versus WT. MCV, mean corpuscular volume; MCH, mean corpuscular hemoglobin; MCHC, MCH concentration.



**Figure 3**

$\beta_3$ (Y747A) and  $\beta_3$ (L746A) mice are protected from microvascular thrombosis. (A) Mice were injected intravenously with 800  $\mu\text{g}/\text{kg}$  collagen and 60  $\mu\text{g}/\text{kg}$  epinephrine and monitored for 30 minutes. \* $P < 0.005$ . (B) Representative sections of H&E-stained lungs from a WT mice that died during the assay and  $\beta_3$ (Y747A) and  $\beta_3$ (L746A) mice that survived and were sacrificed immediately following the assay. WT sections show extensive microthrombi throughout the lungs, while  $\beta_3$  mutant lungs were clear. Scale bars: 200  $\mu\text{m}$  (upper panel); 100  $\mu\text{m}$  (lower panel).

bleeding diathesis similar to that reported for  $\beta_3$ -null animals. On the other hand,  $\beta_3$ (L746A) mice were much less predisposed to these pathologies or to reduced survival.

The foregoing results indicated that the  $\beta_3$ (L746A) mice were protected from thrombosis yet were spared the frequent occurrence of GI bleeding and reduced survival observed in  $\beta_3$ (Y747A) and  $\beta_3$ -null mice. To examine the ability of these animals to achieve hemostasis following injury, we measured the time required to arrest bleeding following tail resection. Both  $\beta_3$ (Y747A) and  $\beta_3$ (L746A) animals manifested impaired hemostasis as evidenced by failure to arrest bleeding within 10 minutes compared with an average of 90 seconds in WT animals (Figure 5C). Thus, while spontaneous GI bleeding is markedly reduced in  $\beta_3$ (L746A) animals, both  $\beta_3$ (Y747A) and  $\beta_3$ (L746A) animals showed impaired hemostasis in a tail bleeding assay.

**Disrupted inside-out signaling in platelets from  $\beta_3$  mutant mice.** To explore the cellular basis for the biological effects of the  $\beta_3$ (Y747A) and  $\beta_3$ (L746A) mutations in mice, we evaluated agonist-induced activation of  $\alpha_{\text{IIb}}\beta_3$  by measuring fibrinogen binding to platelets. As expected, WT  $\beta_3$  mice showed a large increase in the amount of specifically bound fibrinogen in response to ADP/epinephrine, PMA, or a PAR4 thrombin receptor agonist peptide (Figure 6A).  $\beta_3$ (Y747A) and  $\beta_3$ (L746A) platelets showed profoundly impaired responses. In contrast,  $\beta_3$ (Y747A) and  $\beta_3$ (L746A) platelets bound fibrinogen somewhat better than WT  $\beta_3$  platelets in the presence of 0.5 mM  $\text{MnCl}_2$ , an exogenous activator of the integrin (Figure 6B, left panel). This increased binding was accounted for by a modest increase in  $\beta_3$  integrin surface expression in  $\beta_3$ (Y747A) and  $\beta_3$ (L746A) compared with control platelets (Figure 6B, right panel). Neither platelets preincubated with the  $\beta_3$ -blocking antibody 1B5 nor  $\beta_3$ -null platelets bound fibrinogen in response to the agonists, indicating that the fibrinogen binding was depen-

dent on the  $\beta_3$  integrin (data not shown). Consistent with the fibrinogen-binding defects observed, agonist-induced platelet aggregation was impaired in both mutants (Figure 6C). It is noteworthy that similar functional impairments were observed with selective disruption of talin binding to  $\beta_3$ (L746A) and a near complete blockade of cytoplasmic protein binding to  $\beta_3$ (Y747A). This provides additional evidence for the critical and selective role of talin in this process. Thus, these mutant  $\alpha_{\text{IIb}}\beta_3$  integrins are defective in their capacity to respond with increased affinity to intracellular signals rather than in their innate capacity to bind fibrinogen.

Consistent with preservation of  $\alpha_{\text{IIb}}\beta_3$  ligand-binding function, static adhesion of platelets to immobilized fibrinogen was similar in WT,  $\beta_3$ (Y747A), and  $\beta_3$ (L746A) platelets (Figure 6D). Platelet adhesion was markedly reduced by 1B5, an  $\alpha_{\text{IIb}}\beta_3$ -blocking antibody, or in  $\beta_3$ -null platelets, indicating that adhesion is dependent on  $\beta_3$  integrins. These results show that  $\beta_3$  integrins expressed on  $\beta_3$ (Y747A) and  $\beta_3$ (L746A) platelets maintain ligand-binding function and confirm a previous report that  $\alpha_{\text{IIb}}\beta_3$  activation is not required for static adhesion of platelets to fibrinogen (18).

**Intact outside-in signaling in platelets from  $\beta_3$ (L746A) mice.** Once integrins have bound ligand, they can generate biochemical responses, such as activation of Src family kinases and tyrosine phosphorylation of focal adhesion kinase phosphoprotein of 125 kD ( $\text{pp125}^{\text{FAK}}$ ), that result in cell spreading. To examine the ability of  $\beta_3$ (L746A) to mediate this form of signaling, termed *outside-in* signaling, we measured tyrosine phosphorylation of  $\text{pp125}^{\text{FAK}}$  in response to fibrinogen binding to platelets. When washed platelets were resuspended in buffer containing 250  $\mu\text{g}/\text{ml}$  fibrinogen and stimulated by addition of 100  $\mu\text{M}$  ADP/100  $\mu\text{M}$  epinephrine, WT platelets, but not platelets from  $\beta_3$ (L746A) animals, showed an increase in  $\text{pp125}^{\text{FAK}}$  phosphorylation (Figure 7). However, in the presence of 0.5 mM  $\text{MnCl}_2$  to activate  $\alpha_{\text{IIb}}\beta_3$  extrinsically,  $\beta_3$ (L746A) platelets exhibited fibrinogen-dependent  $\text{pp125}^{\text{FAK}}$  phosphorylation similar to that of WT platelets. This indicates that  $\alpha_{\text{IIb}}\beta_3$ (L746A) is able to mediate outside-in signaling when ligated by fibrinogen. Thus, the reduced  $\text{pp125}^{\text{FAK}}$  phosphorylation in  $\beta_3$ (L746A) platelets shown in Figure 7 is ascribable to their failure to increase fibrinogen binding in response to ADP/epinephrine.  $\beta_3$ (L746A) platelets showed reduced spreading on fibrinogen in response to ADP or PMA (Figure 8). In the presence of  $\text{MnCl}_2$ , however, spreading was similar in WT and  $\beta_3$ (L746A) platelets. Together, these data indicate that blocking talin binding to  $\beta_3$  inhibits  $\alpha_{\text{IIb}}\beta_3$  activation but maintains outside-in signaling and platelet spreading if the  $\alpha_{\text{IIb}}\beta_3$  is activated exogenously.

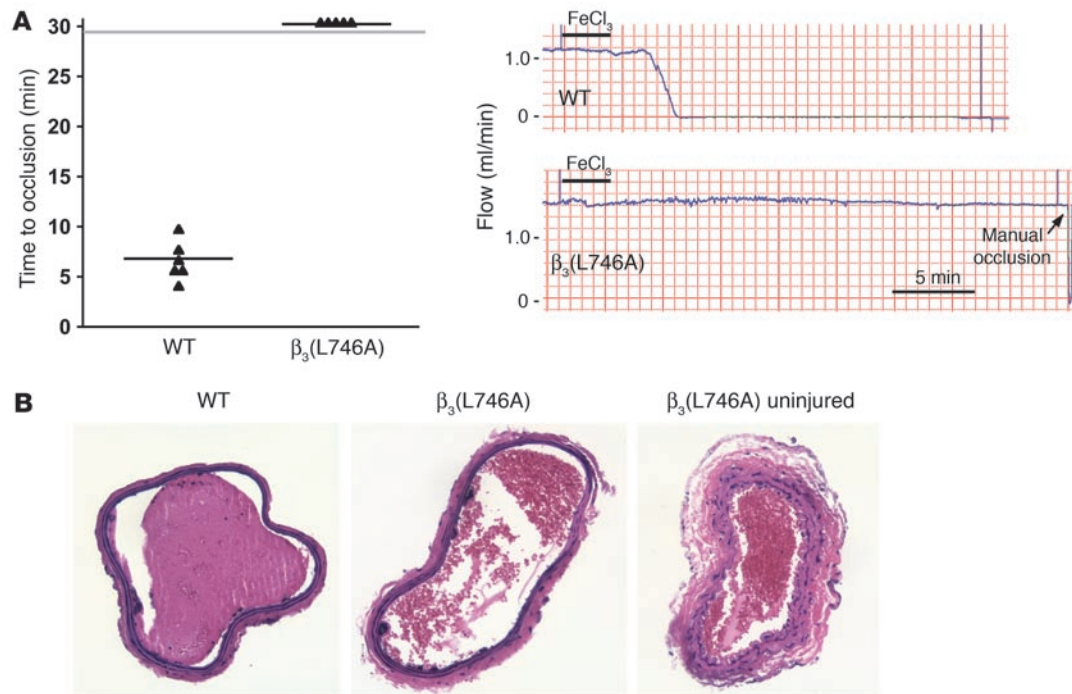


**Figure 4**

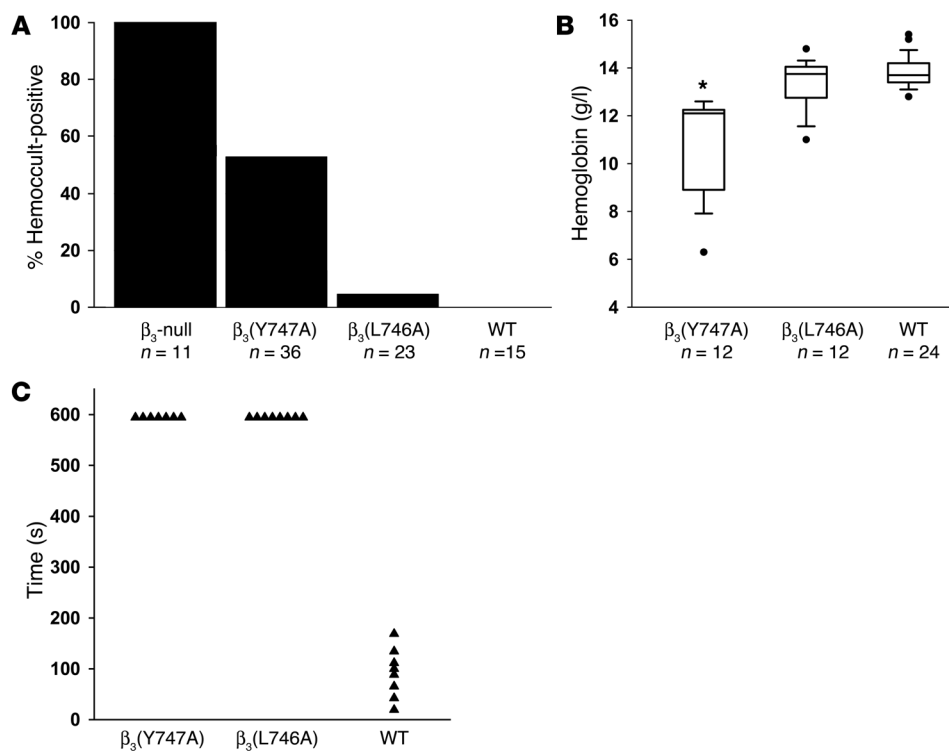
$\beta_3$ (L746A) mice are protected from arterial thrombosis. **(A)** Thrombosis was induced in the carotid artery of mice by a 3-minute application of 5% ferric chloride to the surface of the vessel. The time to complete vessel occlusion was considered the time after injury to zero blood flow as measured with a Doppler flow probe. Representative Doppler flow tracings from a WT and a  $\beta_3$ (L746A) mouse are shown. **(B)** H&E-stained sections of carotid arteries of WT and  $\beta_3$ (L746A) mice obtained 30 minutes after ferric chloride injury. A section of  $\beta_3$ (L746A) carotid artery distal to the injury is shown for comparison. Original magnification,  $\times 200$ .

**Discussion**

Here we have tested the importance of talin binding to integrin  $\beta_3$  in the activation of platelet  $\alpha_{IIb}\beta_3$  and in hemostasis and thrombosis. Guided by insights derived from structural studies of the interactions between the  $\beta_3$  integrin cytoplasmic domain and cytoplasmic proteins, we have generated 2 mouse strains bearing  $\beta_3$  mutations that disrupt talin binding. One strain bears  $\beta_3$ (Y747A), a mutation that disrupts multiple protein interactions with the  $\beta_3$  integrin cytoplasmic domain; the second bears  $\beta_3$ (L746A), a mutation that selectively disrupts  $\beta_3$  integrin–talin interactions. Both strains of mutant mice were protected from pulmonary thrombosis following intravenous injection of collagen and epinephrine. In addition,  $\beta_3$ (L746A) animals showed protection from ferric chloride–induced thrombosis of the carotid artery. Thus, using 2 distinct models of thrombosis, we have established that inhibition of the talin– $\beta_3$  interaction confers an antithrombotic effect. In contrast,  $\beta_3$ (L746A) mice were relatively resistant to the pathological bleeding, as assessed by GI blood loss and anemia, that occurred in 53% of  $\beta_3$ (Y747A) and virtually all  $\beta_3$ -null mice (Figure 5 and ref. 17). Platelets from both  $\beta_3$ (Y747A) and  $\beta_3$ (L746A) mice showed marked reduction in agonist-induced fibrinogen binding to  $\alpha_{IIb}\beta_3$ , providing what we believe to be the first in vivo evidence for the talin dependence of integrin activation in mammals. However, platelet adhesion to immobilized fibrinogen under static conditions was unaffected by either  $\beta_3$  cytoplasmic domain mutation, demonstrating that the  $\alpha_{IIb}\beta_3$  in  $\beta_3$ (Y747A) and  $\beta_3$ (L746A) platelets maintains  $\alpha_{IIb}\beta_3$  ligand binding function. While both mutants showed disrupted activation of  $\alpha_{IIb}\beta_3$ , platelets from the  $\beta_3$ (L746A)

mice were able to spread on fibrinogen and exhibit tyrosine phosphorylation of pp125<sup>FAK</sup> when  $\alpha_{IIb}\beta_3$  was activated exogenously by MnCl<sub>2</sub>. Thus,  $\beta_3$ (L746A) mice have a selective defect in the inside-out signaling required for activation of  $\alpha_{IIb}\beta_3$ , yet their platelets maintain the capacity to generate  $\alpha_{IIb}\beta_3$ -mediated outside-in signals required for platelet spreading. Together, these results establish the importance of the talin– $\beta_3$  integrin interaction in  $\alpha_{IIb}\beta_3$  activation in platelets and show that blocking this interaction can have a potent antithrombotic effect without the kind of pathological bleeding associated with complete lack of  $\alpha_{IIb}\beta_3$  function.

Previous studies using a variety of in vitro approaches showed that talin binding to the  $\beta_3$  integrin cytoplasmic domain induces  $\alpha_{IIb}\beta_3$  activation (10, 11) and is a final common step in the process (12). Platelets bearing  $\beta_3$ (L746A), which leads to specific loss of talin binding, bound significantly less fibrinogen in response to platelet agonists than WT platelets, indicating a marked defect in inside-out signaling (Figure 6). The low levels of fibrinogen binding observed with high agonist doses in  $\beta_3$ (L746A) and  $\beta_3$ (Y747A) mutant platelets may have been due to either incomplete inhibition of talin binding to the integrin or to the existence of a talin-independent  $\alpha_{IIb}\beta_3$  activation mechanism. Truncation of the  $\beta_3$  cytoplasmic domain [ $\beta_3$ (724X); ref. 19] or a point mutation [ $\beta_3$ (S752P)] (20) is associated with defective hemostasis and reduced agonist-mediated  $\alpha_{IIb}\beta_3$  activation in humans; however, the  $\beta_3$ (724X) mutation is expected to block binding of multiple proteins (21), and the binding defect in  $\beta_3$ (S752P) remains to be defined (22). Furthermore, in contrast to  $\beta_3$ (L746A), the 2 human mutations impair outside-in signaling (23, 24). Our results are

**Figure 5**

Bleeding diathesis in  $\beta_3$  mutant mice. **(A)** The presence of fecal blood was detected using a guaiac-based hemocult test. Fecal specimens obtained from the indicated genotypes of mice at 6–12 weeks of age were scored as positive or negative in a blinded manner. **(B)** Box plot showing hemoglobin concentration measured in peripheral blood. Filled circles represent outliers and were included in statistical analysis. \* $P < 0.05$  compared with WT. **(C)** Tail bleeding times.  $\beta_3$ (Y747A) and  $\beta_3$ (L746A) homozygotes showed bleeding times of at least 10 minutes (at which time bleeding was stopped by cauterization), while WT mice showed significantly shorter bleeding times.

complemented by the subtle hemostatic and platelet function defects observed in mice bearing  $\beta_3$ (Y747,759F) mutations. Those mice display a defect in secondary platelet aggregation ascribed to defective outside-in signaling and manifest rebleeding from tail wounds after initial hemostasis (16). The  $\beta_3$ (Y747,759F) mutation does not block talin binding, and platelets from those animals manifested normal agonist-induced activation of integrin  $\alpha_{IIb}\beta_3$  and primary hemostasis. In contrast, as noted above, the  $\beta_3$ (L746A) and  $\beta_3$ (Y474A) mice showed defective  $\alpha_{IIb}\beta_3$  activation, impaired primary aggregation, and prolonged bleeding times. Because of these differences in functional effects, it would be of great interest to examine the impact of the  $\beta_3$ (Y747,759F) mutations in comparison to the dramatic effect of the  $\beta_3$ (L746A) mutation on platelet-dependent thrombosis.

The importance of talin binding for integrin activation *in vivo* is likely to apply to other integrins. The critical structural features for talin binding are conserved in multiple mammalian ( $\beta_1$ ,  $\beta_2$ ,  $\beta_3$ ,  $\beta_5$ ,  $\beta_6$ ,  $\beta_7$ ) integrins and in invertebrate integrins (13). Previous *in vitro* studies indicate that talin participates in the activation of  $\beta_1$  and  $\beta_2$  integrins (12, 25, 26). Mice bearing  $\beta_1$ (Y783,795A) manifest defective  $\beta_1$  integrin activation in keratinocytes and platelets (27, 28).  $\beta_1$ (Y783A) is known to disrupt talin binding to  $\beta_1$  (14); hence, the defective activation of  $\beta_1$ (Y783,795A) integrins is consistent with a general role for talin in activation of  $\beta_1$  integrins *in vivo*. Nevertheless, as shown in Figure 1, a tyrosine-to-alanine substitution at this position within the  $\beta_3$  integrin (or a homologous mutation in  $\beta_1$  integrin; ref. 14) disrupts many protein interactions with the  $\beta$  integrin cytoplasmic domain. Thus, the results from the  $\beta_3$ (L746A) mutant mouse reported here, harboring a mutation that selectively disrupts  $\beta_3$  integrin–talin interactions, unambiguously demonstrate that talin binding to the integrin  $\beta$  cytoplasmic domain is critical for *in vivo* integrin activation.

Blockade of talin binding to  $\alpha_{IIb}\beta_3$  inhibits thrombosis with less pathological bleeding than complete lack of  $\alpha_{IIb}\beta_3$  function. Loss of  $\alpha_{IIb}\beta_3$  in humans, due to mutation in either  $\alpha_{IIb}$  or  $\beta_3$  integrin genes (Glanzmann thrombasthenia) or as the result of pharmacological blockade of ligand binding to  $\alpha_{IIb}\beta_3$ , is associated with an increased risk of pathological bleeding (1, 29). Gene-targeted mice lacking  $\alpha_{IIb}\beta_3$  are protected from thrombosis (30) but manifest a greater than 95% incidence of GI bleeding and are severely anemic (ref. 17 and Figure 5).  $\beta_3$ (L746A) animals displayed negligible GI bleeding or anemia (Figure 5). The ability of  $\beta_3$ (L746A) platelets to adhere to immobilized fibrinogen and to generate outside-in signals may account for the lack of pathological bleeding. The increased GI bleeding in the  $\beta_3$ (Y747A) mice is likely a reflection of the lack of selectivity of  $\beta_3$ (Y747A) for inhibition of binding of cytoplasmic proteins, implying that  $\beta_3$ (Y747A) can disrupt many signaling events in addition to integrin activation (31, 32). Whereas  $\beta_3$ (L746A) animals showed little sign of pathological bleeding, they, like  $\beta_3$ (Y747A) and  $\beta_3$ -null animals, displayed impaired hemostasis in response to tail resection. In  $\beta_3$ (L746A) mice, agonist-induced fibrinogen binding, a key step in aggregation, was blocked, and tail resection resulted in bleeding from medium-sized veins and arteries. Thus,  $\alpha_{IIb}\beta_3$ -mediated platelet aggregation is essential for arrest of bleeding from larger vessels, but the  $\alpha_{IIb}\beta_3$ -mediated adhesion and outside-in signaling may be sufficient for hemostasis in the microcirculation.

The results of this study suggest that blockade of the talin– $\alpha_{IIb}\beta_3$  interaction may offer a therapeutic target in pathological thrombosis. Because ligand binding to integrin  $\alpha_{IIb}\beta_3$  is absolutely required for platelet aggregation,  $\alpha_{IIb}\beta_3$  inhibitors are an effective monotherapy for preventing acute thrombosis in the setting of percutaneous coronary intervention (33). In sharp contrast, chronic blockade of  $\alpha_{IIb}\beta_3$  by orally administered antagonists is ineffective in thrombosis protection, possibly because of the need



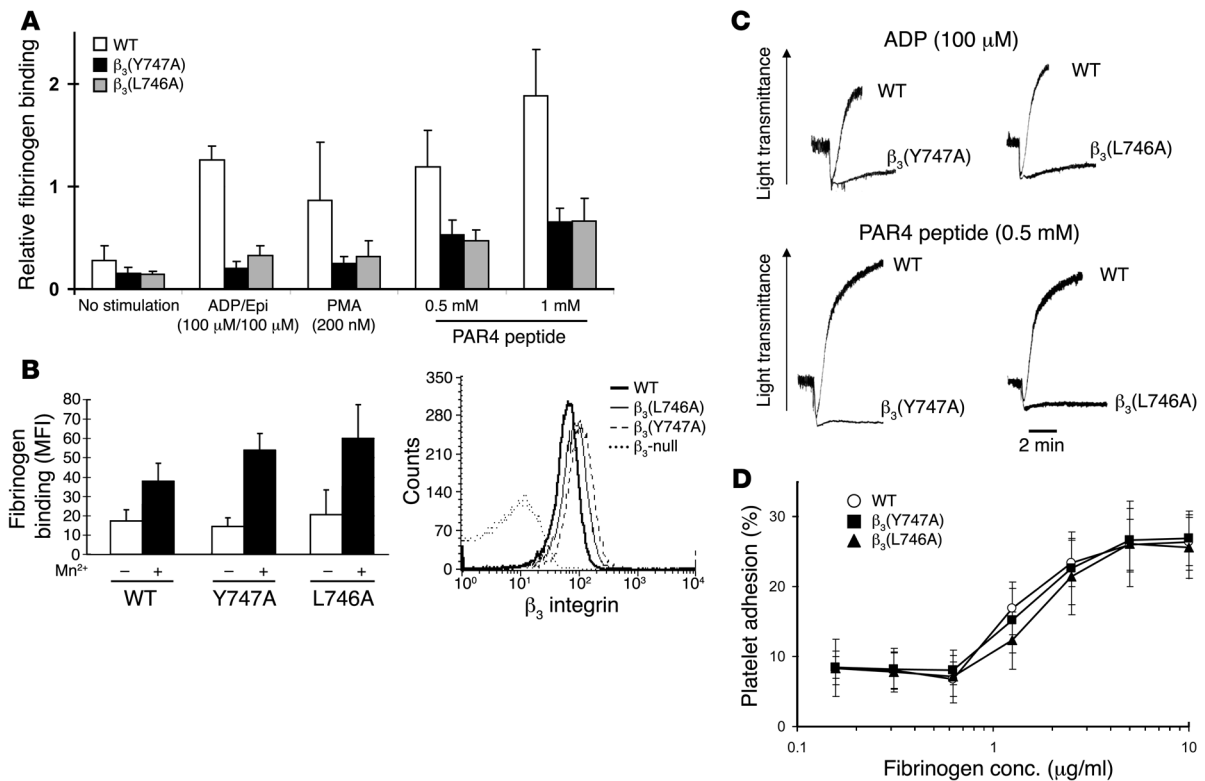


**Figure 6**

$\beta_3$ (Y747A) and  $\beta_3$ (L746A) platelet interactions with fibrinogen. (A) FITC-labeled fibrinogen binding was measured by flow cytometry. Fibrinogen binding was reduced in  $\beta_3$  mutant platelets in response to platelet agonists. Specific binding was defined as that which was inhibitable by 2 mM EDTA. Mean fluorescence intensity (MFI) for each agonist treatment was normalized to the MFI obtained with 0.5 mM MnCl<sub>2</sub> treatment. *n* = 7, 6, and 4 for WT,  $\beta_3$ (Y747A), and  $\beta_3$ (L746A), respectively. Epi, epinephrine. (B) Platelets from both WT mice and  $\beta_3$  mutants showed increased fibrinogen binding in the presence of 0.5 mM MnCl<sub>2</sub> (left). Surface  $\beta_3$  integrin expression of platelets obtained from  $\beta_3$  mutant animals (right). Results are representative of 4 independent experiments and at least 4 mice per genotype. (C) Aggregation of platelets obtained from WT or  $\beta_3$  mutant mice was measured in response to the addition of 100  $\mu$ M ADP or 0.5 mM PAR4 peptide. Results are representative of at least 2 independent experiments on at least 3 animals from each genotype. (D) Platelet adhesion to immobilized fibrinogen. Washed platelets were incubated in fibrinogen-coated microtiter wells for 1 hour at room temperature. Results are shown as percentage of adherent cells relative to the total number added to each well. *n* = 7, 5, and 4 for WT,  $\beta_3$ (Y747A), and  $\beta_3$ (L746A), respectively. Error bars represent SD.

to limit dosage to avoid pathological bleeding (5). Effective oral antithrombotics, such as aspirin or clopidogrel, partially block  $\alpha_{IIb}\beta_3$  activation at the level of an agonist receptor or generation of an endogenous platelet agonist. Here we show that disrupting the  $\beta_3$  integrin–talins interaction blocks  $\alpha_{IIb}\beta_3$  activation and has a dramatic antithrombotic effect and that blocking this interaction leaves the ligand-binding function of platelet  $\alpha_{IIb}\beta_3$  intact. Similarly, inhibiting  $\alpha_{IIb}\beta_3$  activation by agents such as aspirin and clopidogrel also spares the ligand-binding function of  $\alpha_{IIb}\beta_3$ . This preservation of ligand-binding function in combination with preservation of outside-in signaling probably accounts for the markedly diminished pathological bleeding in the  $\beta_3$ (L746A) mice relative to those with complete lack of  $\beta_3$  function. Thus, these studies suggest the principle that the reduction in pathological bleeding associated with blocking the  $\alpha_{IIb}\beta_3$ -talins interaction creates a wider therapeutic window than that achieved by blocking extracellular ligand binding to  $\alpha_{IIb}\beta_3$ . Furthermore, by preventing a final common event leading to integrin activation, disrupting this interaction might prove more effective than currently available oral antiplatelet agents that block a single agonist pathway. Small molecule inhibitors of integrin cytoplasmic domain protein-protein interac-

tions are feasible (34), and the critical structural features of the talin-integrin interaction have been defined (13), suggesting that the principle established here may pave the way to development of a new class of antithrombotic agents.

**Methods**

*Generation of  $\beta_3$ (Y747A) and  $\beta_3$ (L746A) knock-in mice.* A 6-kb fragment of the  $\beta_3$  integrin gene encompassing exons 14 and 15 was amplified from R1 ES cell genomic DNA by PCR and inserted into pBluescript, and its identity was verified by sequencing. Mutations (coding for L746A or Y747A) in exon 15 were inserted by splice-overlap PCR (35) and confirmed by sequencing. A targeting vector was constructed by inserting a phosphoglycerate kinase (PGK) promoter-driven Neo cassette flanked by loxP sequences into a HindIII site between exons 14 and 15 and a PGK-diphtheria toxin A cassette 5' to the  $\beta_3$  sequence (Figure 2A). The targeting sequence was isolated from pBluescript by NotI restriction digestion, agarose gel purified, and electroporated into 129/SvJ ES cells at both the UCSD Transgenic Core Facility and the Fannie E. Rippel Transgenic Facility at the Massachusetts Institute of Technology (MIT). G418-resistant colonies were screened by PCR using primer A (5'-CACTTTGAGGTTTGAGGGTC-3') and primer B (5'-GCTGATCCTCTAGAGTCGAC-3') as depicted in Figure 2A. Positive clones



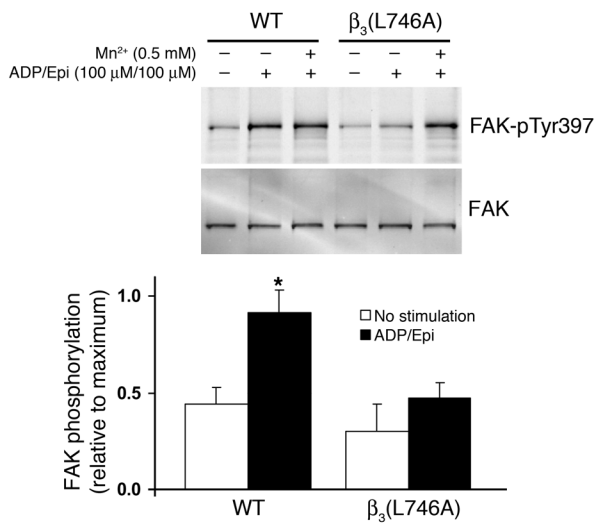


**Figure 7**

pp125<sup>FAK</sup> phosphorylation. Platelets were incubated in suspension with 250  $\mu$ g/ml soluble fibrinogen with or without 0.5 mM MnCl<sub>2</sub> and ADP/epinephrine (100  $\mu$ M each), as indicated, for 20 minutes at room temperature. Platelets were lysed, and pp125<sup>FAK</sup> phosphorylation was measured by immunoblotting using an antibody against pp125<sup>FAK</sup> (pTyr397). Blots were stripped and reprobed with an antibody to pp125<sup>FAK</sup>. Results are shown relative to maximum pp125<sup>FAK</sup> phosphorylation signal for each group. \**P* < 0.05.

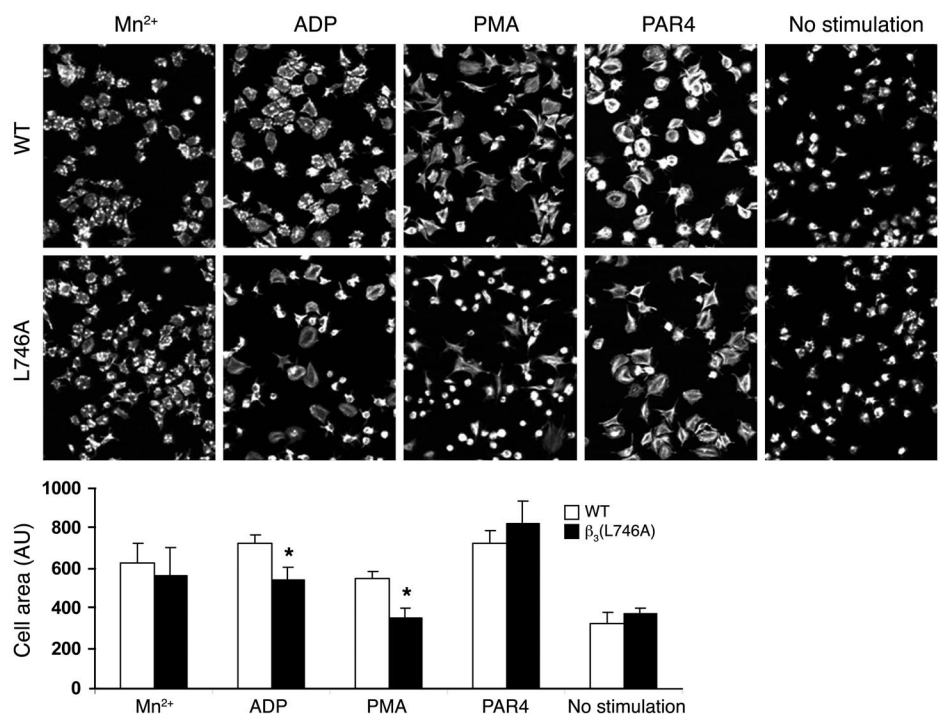
were further analyzed by Southern blotting of BamHI-digested genomic DNA using a 600-bp 5' cDNA probe upstream of the targeted sequence (Figure 2A). This resulted in a 3.2-kb band from the WT allele and a 5.4-kb band from the targeted allele. When genomic DNA was digested with EcoRI and hybridized with a 600-bp 3' cDNA probe complementary to a sequence downstream of the targeted sequence, we expected a 7-kb band from the WT allele and a 9.2-kb band from the targeted allele (Figure 2). Blots were hybridized with a cDNA containing the Neo resistance gene to detect random insertional events of the targeting vector. Positive clones (6 for each mutation), containing a single insertion, were karyotyped, and at least 2 clones for each mutant were injected into C57BL/6 host blastocysts. Chimeric male mice were bred to C57BL/6 females, and agouti offspring from these crosses were genotyped by PCR using genomic DNA extracted from ear biopsies and primer C (5'-CAGTCCTCTACCTTA-

CAGTG-3') and primer D (5'-CTCTGCCCTCAGTTTCCTTA-3') as depicted in Figure 2A. Two independently derived heterozygous animals for each mutation [ $\beta_3$ (Y747A), 1 from MIT and 1 from UCSD; and  $\beta_3$ (Y746A), from UCSD], were crossed with EIIa-Cre mice (The Jackson Laboratory) to delete the Neo cassette in germ cells (36). Deletion of Neo and presence of the targeted allele in offspring from  $\beta_3$  mutant and EIIa-Cre crosses were evaluated by PCR of genomic DNA using primers C and D (Figure 2A). All experiments were performed with independently derived lines for each mutation that were backcrossed to the C57BL/6 strain for at least 3 generations. Sex-matched WT littermates were used as control animals. Mice were housed in the UCSD animal facility, and experiments were approved by the UCSD Institutional Animal Care and Use Committee.

*Molecular modeling.* Modeling was performed using DeepView – Swiss-Pdb viewer (<http://www.expasy.org/spdbv/>; ref. 37).  $\beta_3$  integrin cytoplasmic

**Figure 8**

Agonist-stimulated platelet spreading. Platelets were allowed to spread on fibrinogen-coated coverslips (100  $\mu$ g/ml) in the presence of MnCl<sub>2</sub> (0.5 mM), ADP (100  $\mu$ M), PMA (200 nM), or PAR4 peptide (1 mM), as indicated, for 45 minutes, fixed, and stained with rhodamine-phalloidin. The results were quantified from 2 independent experiments. \**P* < 0.05. Error bars represent SD. Original magnification,  $\times 1,260$ .





domain interactions with filamin A were modeled based on the structure of  $\beta_7$  integrin cytoplasmic domain and filamin A (38). This approach is justified by nuclear magnetic resonance spectroscopy and mutational studies that indicate that these integrin cytoplasmic domains bind to filamin A in a similar manner. Sequence threading was guided using the NPXY motif sequence, which is identical in the  $\beta_3$  and  $\beta_7$  integrins. The resulting sequence alignment was submitted to Swiss-Model (<http://swissmodel.expasy.org>). The resulting model had no major errors as determined by the WhatCheck report on the expasy website.

**Affinity chromatography with recombinant integrin cytoplasmic domains.** Platelets were obtained from WT C57BL/6 mice as described below and lysed as previously described (11). Affinity chromatography was performed using recombinant integrin cytoplasmic domains bound to His-Bind Resin (Novagen) as previously described (11, 14). Samples were separated on a 4%–20% SDS-polyacrylamide gel (Novex; Invitrogen) and transferred for Western blotting with the following antibodies: talin 8d4 (Sigma-Aldrich), anti-filamin A (a kind gift from John Hartwig, Harvard Medical School, Boston, Massachusetts, USA), and c-Src and Syk (Santa Cruz Biotechnology Inc.). Signal was detected and results quantified using an Odyssey imaging system (LI-COR Biosciences).

**Thrombosis assays.** Pulmonary thromboembolism experiments were performed as described previously (39). Briefly, mice under isoflurane anesthesia were administered 200  $\mu$ l of saline containing 0.8 mg/kg collagen (Chrono-log Corp.) and 60  $\mu$ g/kg epinephrine via tail vein injection. Animals were monitored for death as determined by cessation of breathing for up to 30 minutes after injection. Lungs were removed, fixed overnight with 10% neutral buffered formalin, and embedded in paraffin. Sections were stained with H&E, and images were captured with a Leica DM LS microscope and Spot color digital camera (National Diagnostics).

Ferric chloride-induced thrombosis was induced as previously described (40) by applying a 1.2  $\times$  1.2-mm piece of filter paper soaked in 5% ferric chloride to each side of the common carotid artery of a mouse under isoflurane anesthesia. After 3 minutes, the filter paper was removed and the vessel was washed twice with saline. Flow through the carotid artery was monitored 2 minutes before injury and at least 30 minutes after removal of the ferric chloride using a 0.5 PSB Doppler flow probe and T402 flowmeter (Transonic Systems Inc.). Following the assay, the artery was ligated with sutures to stop the flow of blood, and the artery was removed, fixed in 3.7% formaldehyde, embedded in paraffin, sectioned, and stained with H&E.

**Hemostasis assays.** The presence of fecal blood was assessed with a guaiac-based hemocult detection assay (Helena Laboratories) on freshly obtained stool samples. Tail bleeding assays were performed by resecting 1 mm of the tail followed by immersion in 37°C isotonic saline (17). All experiments were terminated at 10 minutes by cauterizing the tail.

**Blood counts.** Peripheral blood was collected from the retro-orbital plexus and transferred to tubes containing EDTA. Cell counts were performed using an MS9 automated cell counter (Melet Schloesing Laboratories) with veterinary parameters and reagents. Differential counts were performed manually on Wright-Giemsa-stained smears. Box-and-whisker plots of hemoglobin concentration were generated in which the box represents an interquartile range (IQR), a horizontal line represents the median, and vertical lines represent 1.5  $\times$  IQR. Outliers are represented by filled circles and were included in statistical analysis.

**Platelet isolation and functional assays.** Washed platelets were obtained from fresh anticoagulated blood and resuspended at 3  $\times$  10<sup>8</sup>/ml in a platelet incu-

bation buffer (41). Soluble fibrinogen binding was performed by incubating platelets for 20 minutes with 150  $\mu$ g/ml FITC-labeled fibrinogen followed by fixation with 1% formaldehyde for 10 minutes at room temperature and analyzed on a FACScan (BD). Surface expression of  $\beta_3$  integrin was measured by flow cytometry using an FITC-conjugated anti-mouse CD61 antibody (BD Biosciences). Platelet aggregation was performed as described previously (17) using platelet-rich plasma (PRP) at a platelet concentration of 3.5  $\times$  10<sup>8</sup> platelets/ml obtained from blood drawn into 0.1-volume 0.13 M sodium citrate. Aggregation of 300  $\mu$ l of PRP was measured at 37°C while stirring using a 2-channel aggregometer (Chrono-log Corp.). Platelet adhesion assays were performed by incubating washed platelets for 1 hour at room temperature in fibrinogen-coated microtiter wells as previously described (42), and platelets were quantified by acid phosphatase assay (41). Platelet spreading was analyzed by confocal microscopy after cells were plated on coverslips coated with 100  $\mu$ g/ml fibrinogen for 45 minutes at room temperature. Platelets were fixed with 4% formaldehyde/PBS for 10 minutes at room temperature and labeled with rhodamine-phalloidin. Images were captured with a Leica SP2 confocal microscope, and cell area was quantified using ImageJ software (version 1.36b; <http://rsb.info.nih.gov/ij/>). To analyze FAK phosphorylation, platelets in suspension were incubated with 250  $\mu$ g/ml fibrinogen with or without 0.5 mM MnCl<sub>2</sub> and ADP/epinephrine (100  $\mu$ M each) for 20 minutes at room temperature. Platelets were then lysed by addition of one-half volume 3 $\times$  lysis buffer (3% NP-40, 450 mM NaCl, 150 mM Tris-HCl, pH 7.4, 3 mM NaVO<sub>4</sub>, 1.5 mM NaF, 3 mM PMSF, 15 mM EDTA, and complete protease inhibitor; Roche) and clarified by centrifugation at 13,000 g for 10 minutes at 4°C. Forty micrograms of protein was separated on 4%–20% Tris-glycine gels (Novex; Invitrogen) and transferred to nitrocellulose membranes for probing with anti-FAK(pTyr397) (Biosource) and FAK antibodies (Santa Cruz Biotechnology Inc.). Signal was detected and results quantified by infrared fluorescence spectrometry using an Odyssey imaging system (LI-COR Biosciences).

**Statistics.** Statistical significance was determined by Student's *t* test for all experiments but the pulmonary thromboembolism study, which was analyzed using Fisher's exact test. A *P* value of less than 0.05 was considered statistically significant.

**Acknowledgments**

We gratefully acknowledge Aurora Burds Connor and Ella Kotheri for excellent assistance in generating gene-targeted animals. We thank Zaverio Ruggeri for valuable discussions concerning the ferric chloride thrombosis model. This work was supported by grants from the NIH (HL57900 and HL078784) and from the Cell Migration Consortium, NIH (U54 GM064346). B.G. Petrich is a postdoctoral fellow of the American Heart Association. A.W. Partridge held a postdoctoral fellowship from the Tobacco-Related Disease Research Program. P. Fogelstrand has a postdoctoral fellowship from the Swedish Research Council.

Received for publication November 21, 2006, and accepted in revised form April 24, 2007.

Address correspondence to: Mark H. Ginsberg, Department of Medicine, University of California, San Diego, 9500 Gilman Drive, mail stop 0726, La Jolla, California 92093-0726, USA. Phone: (858) 822-6432; Fax: (858) 822-6458; E-mail: mhginsberg@ucsd.edu.

1. Quinn, M.J., Byzova, T.V., Qin, J., Topol, E.J., and Plow, E.F. 2003. Integrin alphaIIb beta3 and its antagonist. *Arterioscler. Thromb. Vasc. Biol.* **23**:945–952.  
 2. Chew, D.P., Bhatt, D.L., Sapp, S., and Topol, E.J. 2001. Increased mortality with oral platelet glycoprotein IIb/IIIa antagonists: a meta-analysis of phase III multicenter randomized trials. *Circulation.* **103**:201–206.  
 3. Shattil, S.J., and Newman, P.J. 2004. Integrins: dynamic scaffolds for adhesion and signaling in platelets. *Blood.* **104**:1606–1615.  
 4. Ginsberg, M.H., Partridge, A., and Shattil, S.J. 2005. Integrin regulation. *Curr. Opin. Cell. Biol.* **17**:509–516.  
 5. Bhatt, D.L., and Topol, E.J. 2003. Scientific and



- therapeutic advances in antiplatelet therapy. *Nat. Rev. Drug Discov.* **2**:15–28.
6. Liddington, R.C., and Ginsberg, M.H. 2002. Integrin activation takes shape. *J. Cell Biol.* **158**:833–839.
7. Adair, B.D., et al. 2005. Three-dimensional EM structure of the ectodomain of integrin  $\alpha V\beta 3$  in a complex with fibronectin. *J. Cell Biol.* **168**:1109–1118.
8. Campbell, I.D., and Ginsberg, M.H. 2004. The talin-tail interaction places integrin activation on FERM ground. *Trends Biochem. Sci.* **29**:429–435.
9. Xiao, T., Takagi, J., Collier, B.S., Wang, J.H., and Springer, T.A. 2004. Structural basis for allostery in integrins and binding to fibrinogen-mimetic therapeutics. *Nature.* **432**:59–67.
10. Calderwood, D.A., et al. 2002. The phosphotyrosine binding-like domain of talin activates integrins. *J. Biol. Chem.* **277**:21749–21758.
11. Calderwood, D.A., et al. 1999. The Talin head domain binds to integrin beta subunit cytoplasmic tails and regulates integrin activation. *J. Biol. Chem.* **274**:28071–28074.
12. Tadokoro, S., et al. 2003. Talin binding to integrin beta tails: a final common step in integrin activation. *Science.* **302**:103–106.
13. Garcia-Alvarez, B., et al. 2003. Structural determinants of integrin recognition by talin. *Mol. Cell.* **11**:49–58.
14. Pfaff, M., Liu, S., Erle, D.J., and Ginsberg, M.H. 1998. Integrin beta cytoplasmic domains differentially bind to cytoskeletal proteins. *J. Biol. Chem.* **273**:6104–6109.
15. Ulmer, T.S., Yaspan, B., Ginsberg, M.H., and Campbell, I.D. 2001. NMR analysis of structure and dynamics of the cytosolic tails of integrin alpha IIb beta 3 in aqueous solution. *Biochemistry.* **40**:7498–7508.
16. Law, D.A., et al. 1999. Integrin cytoplasmic tyrosine motif is required for outside-in  $\alpha IIb\beta 3$  signaling and platelet function. *Nature.* **401**:808–811.
17. Hodivala-Dilke, K.M., et al. 1999.  $\beta 3$ -integrin-deficient mice are a model for Glanzmann thrombasthenia showing placental defects and reduced survival. *J. Clin. Invest.* **103**:229–238.
18. Savage, B., Shattil, S.J., and Ruggeri, Z.M. 1992. Modulation of platelet function through adhesion receptors. A dual role for glycoprotein IIb-IIIa (integrin alpha IIb beta 3) mediated by fibrinogen and glycoprotein Ib-von Willebrand factor. *J. Biol. Chem.* **267**:11300–11306.
19. Wang, R., Shattil, S.J., Ambruso, D.R., and Newman, P.J. 1997. Truncation of the cytoplasmic domain of  $\beta 3$  in a variant form of Glanzmann thrombasthenia abrogates signaling through the integrin  $\alpha IIb\beta 3$  complex. *J. Clin. Invest.* **100**:2393–2403.
20. Chen, Y.P., et al. 1992. Ser-752→Pro mutation in the cytoplasmic domain of integrin beta 3 subunit and defective activation of platelet integrin alpha IIb beta 3 (glycoprotein IIb-IIIa) in a variant of Glanzmann thrombasthenia. *Proc. Natl. Acad. Sci. U. S. A.* **89**:10169–10173.
21. Liu, S., Calderwood, D.A., and Ginsberg, M.H. 2000. Integrin cytoplasmic domain-binding proteins. *J. Cell Sci.* **113**:3563–3571.
22. Ma, Y.Q., et al. 2006. Regulation of integrin  $\alpha IIb\beta 3$  activation by distinct regions of its cytoplasmic tails. *Biochemistry.* **45**:6656–6662.
23. Chen, Y.P., O'Toole, T.E., Ylanne, J., Rosa, J.P., and Ginsberg, M.H. 1994. A point mutation in the integrin beta 3 cytoplasmic domain (S752→P) impairs bidirectional signaling through alpha IIb beta 3 (platelet glycoprotein IIb-IIIa). *Blood.* **84**:1857–1865.
24. Ylanne, J., et al. 1993. Distinct functions of integrin alpha and beta subunit cytoplasmic domains in cell spreading and formation of focal adhesions. *J. Cell Biol.* **122**:223–233.
25. Kim, M., Carman, C.V., and Springer, T.A. 2003. Bidirectional transmembrane signaling by cytoplasmic domain separation in integrins. *Science.* **301**:1720–1725.
26. Kuo, J.C., Wang, W.J., Yao, C.C., Wu, P.R., and Chen, R.H. 2006. The tumor suppressor DAPK inhibits cell motility by blocking the integrin-mediated polarity pathway. *J. Cell Biol.* **172**:619–631.
27. Chen, H., et al. 2006. In vivo beta1 integrin function requires phosphorylation-independent regulation by cytoplasmic tyrosines. *Genes Dev.* **20**:927–932.
28. Czuchra, A., Meyer, H., Legate, K.R., Brakebusch, C., and Fassler, R. 2006. Genetic analysis of beta1 integrin “activation motifs” in mice. *J. Cell Biol.* **174**:889–899.
29. George, J.N., Caen, J.P., and Nurden, A.T. 1990. Glanzmann's thrombasthenia: the spectrum of clinical disease. *Blood.* **75**:1383–1395.
30. Smyth, S.S., Reis, E.D., Vaananen, H., Zhang, W., and Collier, B.S. 2001. Variable protection of beta 3-integrin-deficient mice from thrombosis initiated by different mechanisms. *Blood.* **98**:1055–1062.
31. Tahiliani, P.D., Singh, L., Auer, K.L., and LaFlamme, S.E. 1997. The role of conserved amino acid motifs within the integrin beta3 cytoplasmic domain in triggering focal adhesion kinase phosphorylation. *J. Biol. Chem.* **272**:7892–7898.
32. Woodside, D.G., et al. 2001. Activation of Syk protein tyrosine kinase through interaction with integrin beta cytoplasmic domains. *Curr. Biol.* **11**:1799–1804.
33. Collier, B.S. 2001. Anti-GPIIb/IIIa drugs: current strategies and future directions. *Thromb. Haemost.* **86**:427–443.
34. Ambroise, Y., Yaspan, B., Ginsberg, M.H., and Boger, D.L. 2002. Inhibitors of cell migration that inhibit intracellular paxillin/alpha4 binding: a well-documented use of positional scanning libraries. *Chem. Biol.* **9**:1219–1226.
35. Ho, S.N., Hunt, H.D., Horton, R.M., Pullen, J.K., and Pease, L.R. 1989. Site-directed mutagenesis by overlap extension using the polymerase chain reaction. *Gene.* **77**:51–59.
36. Lakso, M., et al. 1996. Efficient in vivo manipulation of mouse genomic sequences at the zygote stage. *Proc. Natl. Acad. Sci. U. S. A.* **93**:5860–5865.
37. Guex, N., and Peitsch, M.C. 1997. SWISS-MODEL and the Swiss-PdbViewer: an environment for comparative protein modeling. *Electrophoresis.* **18**:2714–2723.
38. Kiema, T., et al. 2006. The molecular basis of filamin binding to integrins and competition with talin. *Mol. Cell.* **21**:337–347.
39. DiMinno, G., and Silver, M.J. 1983. Mouse antithrombotic assay: a simple method for the evaluation of antithrombotic agents in vivo. Potentiation of antithrombotic activity by ethyl alcohol. *J. Pharmacol. Exp. Ther.* **225**:57–60.
40. Konstantinides, S., Schafer, K., Thinnies, T., and Loskutoff, D.J. 2001. Plasminogen activator inhibitor-1 and its cofactor vitronectin stabilize arterial thrombi after vascular injury in mice. *Circulation.* **103**:576–583.
41. Law, D.A., et al. 1999. Genetic and pharmacological analyses of Syk function in  $\alpha IIb\beta 3$  signaling in platelets. *Blood.* **93**:2645–2652.
42. Arias-Salgado, E.G., et al. 2005. PTP-1B is an essential positive regulator of platelet integrin signaling. *J. Cell Biol.* **170**:837–845.